

## A NOTE ON THE IMPULSE DUE TO A VAPOUR BUBBLE NEAR A BOUNDARY

J. R. BLAKE and P. CERONE

(Received 26 February 1981)

### Abstract

An expression for the impulse due to a vapour (cavitation) bubble is obtained in terms of an integral over a nearby boundary. Examples for a point source near a free surface, rigid boundary, inertial boundary and a fluid of different density are considered. It appears that the sign of the impulse determines the direction a cavitation bubble will migrate and the direction of the high speed liquid jet during the collapse phase. The theory may explain recent observations on buoyant bubbles near an interface between two fluids of different densities.

### 1. Introduction

Cavitation damage to turbo-machinery is a major concern to hydraulic engineers. One of the mechanisms causing damage is the 'pitting' due to a high speed liquid jet impacting on the rigid boundary. However, for a free surface or a suitably pliable surface, the jet is directed away from the surface. In this paper we consider the correlation between the sign of the bubble impulse and the direction of movement of the bubble and the high speed liquid jet near different types of plane boundaries: for example a free surface, an interface between two fluids of different density, a boundary with a prescribed mass per unit area (inertial boundary) and a rigid boundary. It is suggested that the response of both the bubble and the boundary depends on the inertia of the boundary relative to that of the fluid containing the vapour bubble.

A natural extension of the study on the impulse is in its use as a check on the global conservation of linear momentum. Global balances for mass and energy

are generally used as checks on the numerical solution of integral equations in fluid mechanics (see, for example, Longuet-Higgins and Cokelet [12], Fenton and Mills [7]) but linear and angular momentum less frequently. In recent numerical studies of the growth and collapse of vapour (cavitation) bubbles near different boundaries (Blake and Gibson [5], Gibson and Blake [9]) the calculation of the impulse was used for global checks on the approximate numerical solution of the integral equations.

It is well known that there is no force acting on a body in steady flow in an infinite inviscid fluid in the absence of circulation (d'Alembert's paradox). However, it is not so well known that d'Alembert's paradox may not hold in the case of a deformable body in an infinite fluid. Examples of cases where a body may propel itself through a fluid have been presented by Benjamin and Ellis [3], Saffman [13] and more recently Wu [14]. Wu formally develops a mathematical relationship between the impulse due to a deformable body in an infinite fluid and the forces acting on it. In this paper we seek to extend Wu's analysis to a cavitation bubble in a semi-infinite fluid and to illustrate the results with several examples of a source immediately adjacent to different types of boundary. In addition, the theory developed in the paper helps explain some very recent observations on the growth and collapse of cavitation bubbles near flexible boundaries (Gibson and Blake [9]) and the interface between fluids of different density (Chahine and Bovis [6]).

## 2. Derivation of impulse

The linear momentum  $\mathbf{P}$  of a volume  $V$ , surface  $S'$  and unit outward normal  $\mathbf{n}$  of fluid of constant density  $\rho$  is defined as follows:

$$\mathbf{P} = \rho \int_V \mathbf{u} dV = \rho \int_V \nabla \phi dV = \rho \int_{S'} \phi \mathbf{n} dS. \quad (1)$$

Here, we are assuming that we have inviscid potential flow and that we can define the velocity as a gradient of a scalar potential satisfying Laplace's equation.

In the theory to be developed in this section for a vapour bubble near a boundary in a semi-infinite fluid, the material surface  $S'$  will be divided into three separate surfaces: (i) the bubble surface  $S$ , and a material control surface of (ii) the approximately planar boundary  $\Sigma_b$  to the half space and (iii) the outer boundary  $\Sigma$  (see Figure 1). We now write the fluid momentum  $\mathbf{P}$  as the sum of two integrals

$$\mathbf{P} = \rho \left\{ \int_S + \int_{\Sigma \cup \Sigma_b} \right\} \phi \mathbf{n} dS = \mathbf{I}_S + \mathbf{I}_\Sigma. \quad (2)$$

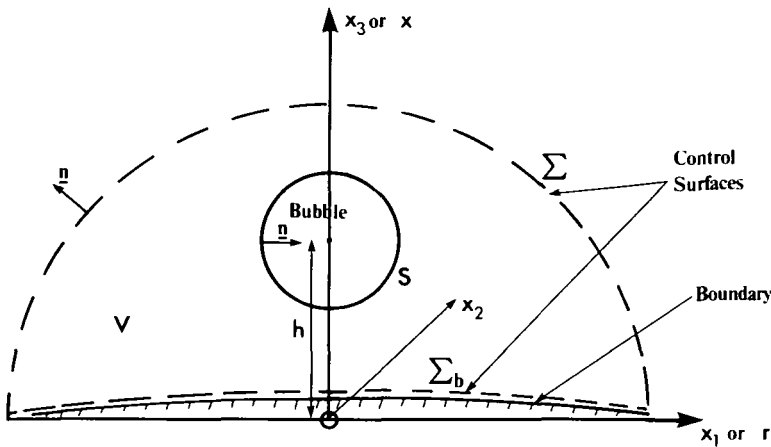


Fig. 1. Geometry and surface described in text.

The lower half-space boundary  $\Sigma_b$  need not be coincident with the plane  $x = 0$ .

Clearly in the case of a cavitation bubble, the potential will have a source-like behaviour and hence  $\phi$  will vary inversely with distance. If the outer control surface is allowed to extend to infinity, the expression for the fluid momentum normally yields a divergent integral (the exceptions being the infinite fluid and the linearised free surface examples). The solution to this dilemma is to consider the rate of change of the fluid momentum in a finite volume  $V$  which must be equal to the force  $\mathbf{F}$  acting on the fluid, either at the external boundaries or due to a buoyancy force (Landau and Lifshitz [11]), as follows:

$$\frac{d\mathbf{P}}{dt} = \mathbf{F}. \tag{3}$$

Omitting buoyancy forces for the moment and considering the remaining surface pressure forces, we have

$$\frac{d\mathbf{P}}{dt} = - \left\{ \int_S + \int_{\Sigma \cup \Sigma_b} \right\} p \mathbf{n} dS. \tag{4}$$

The first integral on the right of (4) can be omitted since the pressure  $p$  is a constant (and equals  $p_c$  the vapour pressure) evaluated over a closed surface. Using the expression for  $\mathbf{P}$  given in (2), we obtain, upon rearranging (4),

$$\frac{d\mathbf{I}_S}{dt} = - \int_{\Sigma \cup \Sigma_b} p \mathbf{n} dS - \frac{d}{dt} \left\{ \rho \int_{\Sigma \cup \Sigma_b} \phi \mathbf{n} dS \right\}. \tag{5}$$

As the outer control boundary  $\Sigma \cup \Sigma_b$  is a material surface, we may use the general surface integral relation defined in Batchelor [2] (page 134) and for this particular example yielding,

$$\frac{d}{dt} \left\{ \rho \int_{\Sigma \cup \Sigma_b} \phi \mathbf{n} dS \right\} = \rho \int_{\Sigma \cup \Sigma_b} \frac{D\phi}{Dt} \mathbf{n} dS - \rho \int_{\Sigma \cup \Sigma_b} \phi \frac{\partial}{\partial n} (\nabla \phi) dS, \tag{6}$$

where  $\frac{D}{Dt}$  is the substantial derivative. On substitution of (6) and the Bernoulli pressure expression

$$p = p_\infty - \rho \frac{\partial \phi}{\partial t} - \frac{1}{2} \rho |\mathbf{u}|^2 \tag{7}$$

into (5), we obtain

$$\frac{d\mathbf{I}_S}{dt} = \rho \int_{\Sigma \cup \Sigma_b} \left( \phi \frac{\partial(\nabla \phi)}{\partial n} - \frac{1}{2} |\nabla \phi|^2 \mathbf{n} \right) dS. \tag{8}$$

Now noting that  $\phi = O(1/R)$  and by letting  $\Sigma$  be extended to large  $R$  we see that the integral over  $\Sigma$  is  $O(1/R^2)$ . On taking the infinite limit, the value of this integral is zero and we are therefore left with the integral over the boundary surface  $\Sigma_b$ . Upon integration, we obtain the expression for the bubble impulse

$$\mathbf{I}_S = \int_0^t \mathbf{F}_e(t) dt, \tag{9a}$$

where

$$\mathbf{F}_e(t) = \rho \int_{\Sigma_b} \left\{ \phi \frac{\partial(\nabla \phi)}{\partial n} - \frac{1}{2} |\nabla \phi|^2 \mathbf{n} \right\} dS. \tag{9b}$$

Thus, we now have a relation between the bubble impulse and an integral over the boundary surface  $\Sigma_b$ . By rearranging (9b) and with the knowledge that  $\phi$  is harmonic, we can also obtain the following equivalent expression for  $\mathbf{F}_e(t)$ :

$$\mathbf{F}_e(t) = \rho \int_{\Sigma_b} \left\{ \frac{1}{2} |\nabla \phi|^2 \mathbf{n} - \frac{\partial \phi}{\partial n} \nabla \phi \right\} dS. \tag{9c}$$

In the next section this expression will be used to obtain the impulse for various singular source solutions corresponding to different (linear) boundary conditions. It appears that the sign of the impulse determines the direction that the cavitation bubble will migrate. In the linear analysis to follow we choose  $x = 0$  to be the boundary surface  $\Sigma_b$ , then the expression for  $\mathbf{F}_e(t)$  in the  $x$ -direction becomes (in cylindrical coordinates)

$$F_x(t) = \mathbf{F}_e(t) \cdot \mathbf{e}_x = \rho \pi \int_0^\infty r(u^2 - v^2) dr, \tag{10}$$

where  $\mathbf{e}_x$  is the unit vector in the  $x$ -direction and  $u$  and  $v$  are the velocities in the  $x$  and  $r$ -directions respectively.

The expressions for  $F_e(t)$  may also be defined as an integral over  $S$  by using the identity

$$\int_S + \int_{\Sigma \cup \Sigma_b} \left\{ \phi \frac{\partial(\nabla \phi)}{\partial n} - \frac{1}{2} |\nabla \phi|^2 \mathbf{n} \right\} dS = 0 \tag{11}$$

which, on substitution into (9b), yields

$$F_e(t) = -\rho \int_S \left\{ \phi \frac{\partial(\nabla \phi)}{\partial n} - \frac{1}{2} |\nabla \phi|^2 \mathbf{n} \right\} dS. \tag{12}$$

This is self consistent, since we would also obtain (12) if we applied the Batchelor formula (6) to  $I_s$  and used the Bernoulli pressure expression on the bubble surface

$$\int_S \left\{ \frac{\partial \phi}{\partial t} + \frac{1}{2} |\nabla \phi|^2 \right\} dS = 0. \tag{13}$$

### 3. Point source-plane boundary examples

Let us suppose we have a point source of strength  $m(t)$  located at the point  $x = h, r = 0$  in the fluid. It is then straightforward to calculate the  $x$ -component of the impulse  $I_x(t)$  by evaluating the integral over the plane boundary ( $x = 0$ ) for the following cases.

#### (a) Rigid boundary

In this case we define the potential  $\phi$  due to a point source as follows:

$$\phi = \frac{-m(t)}{4\pi} \left[ \frac{1}{[(x-h)^2 + r^2]^{1/2}} + \frac{1}{[(x+h)^2 + r^2]^{1/2}} \right]. \tag{14}$$

On the boundary ( $x = 0$ ) we have

$$u = \frac{\partial \phi}{\partial x} = 0 \tag{15a}$$

and

$$v = \frac{\partial \phi}{\partial r} = \frac{mr}{2\pi(r^2 + h^2)^{3/2}}. \tag{15b}$$

On substitution into (9a) and (10) we obtain the following expression:

$$I_x(t) = \frac{-\rho}{16\pi h^2} \int_0^t m^2(t) dt \leq 0. \tag{16}$$

**(b) Free surface** (linearised boundary condition  $\phi = 0$ )

In this case the potential is simply

$$\phi = \frac{-m(t)}{4\pi} \left[ \frac{1}{[(x-h)^2 + r^2]^{1/2}} - \frac{1}{[(x+h)^2 + r^2]^{1/2}} \right]. \quad (17)$$

The velocities on  $x = 0$  are

$$u = \frac{\partial\phi}{\partial x} = -\frac{mh}{2\pi(r^2 + h^2)^{3/2}} \quad (18a)$$

and

$$v = \frac{\partial\phi}{\partial r} = 0. \quad (18b)$$

On substitution into (9a) and (10) we obtain

$$I_x(t) = \frac{\rho}{16\pi h^2} \int_0^t m^2(t) dt \geq 0. \quad (19)$$

We may have anticipated this change from the rigid boundary to free surface example as the law of Bjerknes tells us that an oscillating body will migrate towards a rigid boundary and away from a free surface (Birkhoff and Zarantonello [4]).

**(c) Inertial boundary**

Let us suppose there is some material of mass per unit area  $\sigma$  forming the boundary to the fluid (that is, the boundary has no rigidity). In this case the linearised boundary conditions at  $x = 0$  become

$$\frac{\partial\zeta}{\partial t} = \frac{\partial\phi}{\partial x} \quad (20a)$$

and

$$\sigma \frac{\partial^2\zeta}{\partial t^2} = p_\infty - p, \quad (20b)$$

where  $x = \zeta(r, t)$  is the displacement of the boundary. Equation (20a) is the kinematic condition equating the material velocity to the normal fluid velocity, whereas (20b) is the dynamic boundary condition with the pressure on the non-fluid side being  $p_\infty$ . If we substitute the linearised Bernoulli equation and (20a) into (20b) and integrate we obtain

$$\sigma\phi_x - \rho\phi = 0 \quad \text{on } x = 0. \quad (21)$$

In this case it is convenient to write the solution for a point source in two different ways

$$\phi = \frac{-m(t)}{4\pi} \left[ \frac{1}{[(x-h)^2 + r^2]^{1/2}} + \frac{1}{[(x+h)^2 + r^2]^{1/2}} - 2 \frac{\rho}{\sigma} \int_0^\infty \frac{e^{-\xi(x+h)}}{\xi + \rho/\sigma} J_0(\xi r) d\xi \right] \tag{22a}$$

and

$$\phi = \frac{-m(t)}{4\pi} \left[ \frac{1}{[(x-h)^2 + r^2]^{1/2}} - \frac{1}{[(x+h)^2 + r^2]^{1/2}} + 2 \int_0^\infty \frac{\xi e^{-\xi(x+h)}}{\xi + \rho/\sigma} J_0(\xi r) d\xi \right]. \tag{22b}$$

Here  $J_0$  is a first kind Bessel function of zeroth order. The first two terms in (22a) correspond to the rigid boundary expression for the potential while in (22b) the first two terms correspond to the free surface example. The advantage of the double formulation is that we need only consider the Hankel transforms when we substitute these expressions into (9a) and (10). Thus, for the velocities on  $x = 0$  we have

$$u = \frac{\partial \phi}{\partial x} = \frac{-m(t)\rho/\sigma}{2\pi} \int_0^\infty \frac{\xi e^{-\xi h}}{\xi + \rho/\sigma} J_0(\xi r) d\xi \tag{23a}$$

and

$$v = \frac{\partial \phi}{\partial r} = \frac{m(t)}{2\pi} \int_0^\infty \frac{\xi^2 e^{-\xi h}}{\xi + \rho/\sigma} J_1(\xi r) d\xi, \tag{23b}$$

where  $J_1$  is a Bessel function of first kind and order. On substitution into (9a) and (10), we obtain, for the  $x$ -component of the impulse,

$$I_x(t; \alpha^*) = \frac{\rho H(\alpha^*)}{4\pi h^2} \int_0^t m^2(t) dt, \tag{24a}$$

where

$$H(\alpha^*) = \int_0^\infty r(\alpha^{*2} A^2 - B^2) dr, \tag{24b}$$

$$A = \int_0^\infty \frac{\eta e^{-\eta}}{\eta + \alpha^*} J_0(\eta r) d\eta, \tag{24c}$$

$$B = \int_0^\infty \frac{\eta^2 e^{-\eta}}{\eta + \alpha^*} J_1(\eta r) d\eta, \tag{24d}$$

and  $\alpha^*$  is the following non-dimensional parameter:

$$\alpha^* = \rho h / \sigma. \quad (25)$$

The integrals in (24b, c, d) may be evaluated either (i) numerically after first using an identity from Laplace transform theory to remove the oscillatory behaviour of the Bessel functions and then a transformation of the infinite interval of integration to a finite one or (ii) analytically after using Parseval's formula for Hankel transforms (Keane [10]). The resulting analytic expression for  $H(\alpha^*)$  is as follows:

$$H(\alpha^*) = \alpha^* - 1/4 - 2\alpha^{*2}e^{2\alpha^*}E_1(2\alpha^*), \quad (26)$$

where  $E_1$  is the exponential integral (Abramowitz and Stegun [1]). Using the asymptotic expansions of  $E_1$  for small and large  $\alpha^*$ , we obtain the rigid boundary and free surface limits of  $-0.25$  and  $0.25$  respectively. The graphical solution for  $H(\alpha^*)$  is illustrated in Figure 2. The single zero of  $H(\alpha^*)$  occurs at  $\alpha^* = \alpha_0^* = 0.7798057$  which corresponds to a zero impulse; the same as would be obtained for a simple source in an infinite fluid.

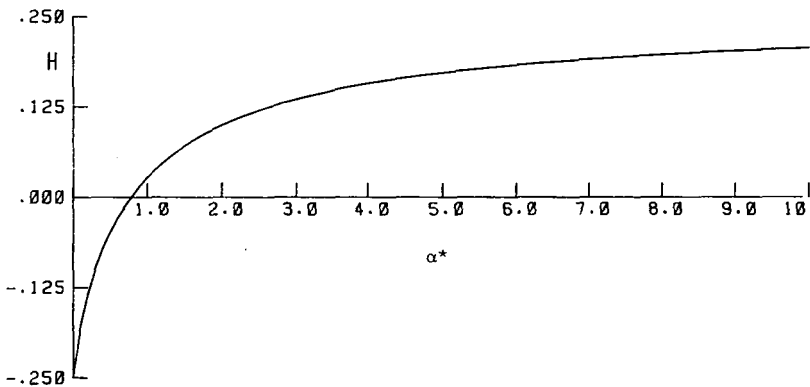


Fig. 2. Graph of  $H$  against  $\alpha^*$  as defined in (26).

Of particular significance is that for  $\alpha^* < \alpha_0^*$  the response of the fluid will tend towards that of a rigid wall whereas for  $\alpha^* > \alpha_0^*$  the behaviour will be more like that of a free surface. In the case of a finite body, such as a cavitation bubble, the potential may be represented by a distribution of sources over the body or along the axis of symmetry. Clearly cases will arise where parts of the bubble may respond as if it is near a rigid boundary whereas in other parts of the bubble the response may tend towards that of a free surface. In the case of the growth and collapse of cavitation bubbles near flexible boundaries, the above discovery may, in part, explain the observations of a cavitation bubble "sticking" to a flexible membrane as reported in Gibson and Blake [9].



**(d) Interface between two fluids**

In this case let us suppose we have two fluids; the lower one with density  $\rho_1$ , the upper fluid with density  $\rho_2$ . If the source is located in the lower fluid at  $x = h$  and if the linearised dynamic boundary condition

$$\rho_1\phi_1 = \rho_2\phi_2 \tag{27}$$

is applied on the interface  $x = 0$ , the expressions for the two potentials are

$$\phi_1 = \frac{-m}{4\pi} \left[ \frac{1}{[(x-h)^2 + r^2]^{1/2}} - \frac{\rho_1 - \rho_2}{\rho_1 + \rho_2} \frac{1}{[(x+h)^2 + r^2]^{1/2}} \right] \tag{28a}$$

and

$$\phi_2 = \frac{-m}{2\pi} \frac{\rho_1}{(\rho_1 + \rho_2)[(x-h)^2 + r^2]^{1/2}}. \tag{28b}$$

On substitution into the expression for the  $x$ -component of the impulse (10), we obtain

$$F_x(t) = \frac{\rho_1 m^2}{16\pi h^2} \frac{(\rho_1 - \rho_2)}{(\rho_1 + \rho_2)}, \tag{29}$$

yielding the expected result for  $\rho_2$  tending to both 0 and  $\infty$  as well as its zero value at  $\rho_1 = \rho_2$  (corresponding to an infinite fluid). This suggests that, in the absence of buoyancy forces on a cavitation bubble, the liquid jet will move in the direction of the denser fluid.

**4. Influence of buoyancy forces**

In a recent paper by Chahine and Bovis [6] on the growth and collapse of a cavitation bubble near the interface between two fluids of different density, the liquid jet was observed to move away from the interface when the cavitation bubble was close to the interface but in the opposite direction when further away. This suggests that buoyancy forces might be influencing the motion of the jet. Indeed Gibson [8] observed and showed that buoyancy forces can alter the direction of the liquid jet.

This can be understood if we include the additional buoyancy force term in the expression for the impulse obtained in (29). Thus we obtain, approximately,

$$F_x(t) = \frac{\rho_1 m^2}{16\pi h^2} \frac{(\rho_1 - \rho_2)}{(\rho_1 + \rho_2)} - (\rho_1 - \rho_c)gV^*, \tag{30}$$

where  $\rho_c$  is the density of the vapour,  $g$  is the gravitational acceleration and  $V^*$  is the instantaneous volume of the cavitation bubble. In this case the source strength  $m$  is approximately  $\frac{dV^*}{dt}$ . It is clear from (30) that for a cavitation bubble of specified size and externally applied pressure that the sign of  $F_x(t)$  will depend on the distance of the centroid from the interface. Thus, if the bubble is close to the interface,  $F_x(t)$  may be positive indicating that the liquid jet will be directed away from the interface whereas further away it will be negative in which case the jet will be directed towards the interface. This theory would therefore suggest that Chahine and Bovis' cavitation bubbles were affected by buoyancy.

## 5. Conclusions

It appears that the sign and magnitude of the bubble impulse may be valuable indicators as to the direction the liquid jet moves during the collapse phase. The larger the magnitude of the impulse, for given bubble volume, the greater the potential for cavitation damage. The impulse appears to predict all previously observed phenomena if we also include buoyancy forces in our calculations.

## Acknowledgements

The authors acknowledge the helpful comments and suggestions made by Dr. D. C. Gibson of the CSIRO Division of Energy Technology and Dr. T. S. Horner of the Department of Mathematics, University of Wollongong.

## References

- [1] M. Abramowitz and I. A. Stegun (eds.), *Handbook of mathematical functions* (Dover, New York, 1965).
- [2] G. K. Batchelor, *An introduction to fluid dynamics* (C.U.P., Cambridge, 1967).
- [3] T. B. Benjamin and A. T. Ellis, "The collapse of cavitation bubbles and the pressures thereby produced against solid bodies", *Phil. Trans. Roy. Soc. (London)* A260 (1966), 221–240.
- [4] G. Birkhoff and E. H. Zarantonello, *Jets, wakes and cavities* (Academic Press, New York, 1957).
- [5] J. R. Blake and D. C. Gibson, "Growth and collapse of a vapour cavity near a free surface", *J. Fluid Mech.* 111(1981), 123–140.
- [6] G. L. Chahine and A. Bovis, "Oscillations and collapse of a cavitation bubble in the vicinity of a two-liquid interface", in *Cavitation and inhomogeneities in underwater acoustics* (ed. W. Lauterborn) (Springer, 1980).

- [7] J. D. Fenton and D. A. Mills, "Shoaling waves: numerical solution of exact equations" in *Waves on water of variable depth* (eds. D. G. Provis and R. Radok), *Lecture Notes in Physics* 64 (Springer, 1976).
- [8] D. C. Gibson, "Cavitation adjacent to plane boundaries", *Proc. 3rd Aust. Hyd. and Fluid Mech. Conf. Sydney* (1968), 210–214.
- [9] D. C. Gibson and J. R. Blake, "Growth and collapse of vapour bubbles near flexible boundaries", *Proc. 7th Aust. Hyd. and Fluid Mech. Conf. Brisbane* (1980), 283–286.
- [10] A. Keane, *Integral transforms* (Science Press, Sydney, 1965).
- [11] L. D. Landau and E. M. Lifshitz, *Fluid mechanics* (Pergamon, Oxford, 1975).
- [12] M. S. Longuet-Higgins and E. D. Cokelet, "The deformation of steep surface waves on water. I A numerical method of computation", *Proc. Roy. Soc. A* 350 (1976), 1–26.
- [13] P. G. Saffman, "The self-propulsion of a deformable body in a perfect fluid", *J. Fluid Mech.* 28 (1967), 385–389.
- [14] T. Y. Wu, "The momentum theorem for a deformable body in a perfect fluid", *Schiffstechnik* 23 (1976), 229–232.

Department of Mathematics  
University of Wollongong  
P. O. Box 1144  
Wollongong  
N.S.W. 2500